X-550-71-224
PREPRINT

A SATELLITE ALTIMETER BIAS RECOVERY SIMULATION

JOHN H. BERBERT
FRED M. LOVELESS

MAY 1971

GSFC
GODDARD SPACE FLIGHT CENTER
GREENBELT, MARYLAND

X-550-71-224

A SATELLITE ALTIMETER BIAS RECOVERY SIMULATION

by

John H. Berbert
Mission Trajectory and Analysis Division
Goddard Space Flight Center

Fred M. Loveless, Jr.
DBA Systems, Inc.

May 1971

Presented in Part at the
GEOS-2 Program Review Meeting
22-24 June 1970

GODDARD SPACE FLIGHT CENTER
Greenbelt, Maryland

A SATELLITE ALTIMETER BIAS RECOVERY SIMULATION

ABSTRACT

Simulations are made for bias recovery of a satellite-borne altimeter by means of data from various combinations of ground-based range and angle measuring systems to determine the accuracy with which the altimeter bias can be recovered under these restricted conditions. Among the parameters considered are the number of stations, station geometry, elevation angle of the pass, and the relative amount of range or range with angle data used. An assessment of the probability of obtaining adequate laser and camera data due to the effect of weather and day or night conditions is included.

The results indicate that, for the systems considered in these simulations, the two station network, with collocated lasers and cameras, is best with respect to accuracy, operational data collection probability, and minimum cost. Such a network is therefore recommended for the satellite altimeter calibration (GEOS-C).

CONTENTS

TABLES

TABLES (continued)

ILLUSTRATIONS

A SATELLITE ALTIMETER BIAS RECOVERY SIMULATION

I. PURPOSE

This altimeter simulation study was initiated to determine how accurately the altitude of a satellite could be determined over short arcs with data from a satellite-borne altimeter and from various combinations of ground based range and angle tracking systems. The tracking stations were chosen to take advantage of existing sites or sites that could be readily equipped. The use of ranging data was assumed at the outset to be essential. Thus, in this simulation, there are never more angle trackers than range trackers. Also the angle trackers, when used, are always collocated at one or more of the ranging sites, as would most likely be the case if the technique is implemented.

The range data a priori bias and rms noise values are chosen to conservatively represent values which were obtained from several lasers and C-band radars during the GEOS-2 tracking system intercomparisons (references 1, 2, 3, 4, 5, 6). The angle data a priori bias and rms noise values represent, somewhat optimistically, values obtained from several cameras intercompared on GEOS-1 (reference 7).

When a Goddard laser was collocated and intercompared with two C-band radars at Wallops Island, (references 1, 2, 3) the results indicated that those C-band radars, when certain calibration and data preprocessing errors were removed, were more or less comparable to that laser in accuracy. Over the last year, however, the laser data rms noise and accuracy has improved by a factor of 2 or 3, and over the next few years is expected to further improve. The C-band radar does have the operational advantage of being able to observe through the clouds. However, in the laser and C-band intercomparisons, the occasional large discrepancies which arose between the systems were always accounted for by some problem with the C-band and not the laser.

From this experience, it seems advisable for an altimeter calibration operation to utilize both the C-band and the laser, the C-band for its operational advantages and the laser to verify the C-band results. For convenience, in this report, the range and angle systems are referred to as lasers and cameras.

This simulation study attempts to answer the following questions:

1. How is the accuracy of the altimeter bias recovery affected by number of lasers and cameras tracking?

2. Is it necessary to have camera data or will the less accurate laser angles provide the directional information?

3. How is the altimeter bias recovery affected by the elevation angle of the satellite pass?

4. How sensitive is the altimeter bias to location of the laser stations?

It is recognized that the answers derived are highly dependent on some of the a priori assumptions, such as the assumed 2 meter ranging accuracy (bias) for the laser. However, the a priori values chosen were thought to be fairly realistic, based on the tests described in the references quoted on page 1. More recent developments indicate that a laser range accuracy of 0.5 meters might now be more realistic.

This study is not intended to provide comprehensive answers to the above questions, but it is hoped the results will be useful in helping to establish a plan for evaluating a satellite-borne altimeter having an overall systems accuracy requirement of 5 meters or better, (reference 8).

Part of the 5 meter overall systems error budget is used up in external errors such as a refraction error, an error due to sea state, and an error due to non-nadir reflection from the sea surface. Consideration of these errors means the calibration system must determine reference heights of the spacecraft altimeter above mean sea level (MSL) to better than 5 meters. For the assumptions made in Reference 9, the required accuracy is 4.1 meters.

II. APPROACH

The study is divided into four cases to answer the four specific questions. In general, the inputs to the computer program are kept either as unconstrained or as realistic as possible. These inputs are such quantities as the orbital elements, station locations, observation uncertainties, observation sampling rate, and error model uncertainties. In all cases, the same orbital elements and observation uncertainties are used.

The four cases are as follows:

Case 1:

The number of laser stations is varied from a minimum of one to a maximum of four. For each number of laser sites, the number of cameras is varied from zero to the number of lasers. The number of cameras is always less than or equal to the number of lasers. The situations are summarized in the following matrix:

CAMERAS:						TRD CUR GTK ANT 4
		0	ANT 1	GTK ANT 2	CUR GTK ANT 3	
LASERS:	ANT 1	(X)	(X)			
	GTK, ANT 2	X	(X)	X		
CUR,	GTK, ANT 3	(X)	X	X	X	
TRD, CUR,	GTK, ANT 4	X	X	X	X	(X)

For each situation, recovery is made for the orbital elements; a constrained range bias for each laser, the constrained survey for each station, and the altimeter bias.

Case 2:

The number of laser stations is varied from one to four. Tracking is simulated with laser azimuth and elevation angles added to the laser ranges in order to determine what advantage the addition of the laser angle data provides over the range data alone.

Case 3:

a. Tracking is simulated for one laser and one camera (1L1C) collocated at the Antigua station. For this station the satellite pass rises to a maximum elevation angle of 87°. Above 20°, the pass is broken into 14 one-minute mini-arc spans of data. Each mini-arc is considered as a separate pass containing both laser and camera data, and recovery is made for the orbital elements, a constrained laser range bias, the constrained station survey, and the altimeter bias. This case, in effect, simulates a geometric recovery for the altimeter bias for various elevation angles, since the mini-arcs contribute very little dynamic constraint to the solution.

b. An altimeter bias is recovered for most of the 14 mini-arcs as in Case 2a. However, the orbital elements, laser range biases, and station surveys are recovered for the total arc. This case shows how the altimeter bias recovery depends on elevation angle when only short spans of altimeter data, but longer spans of comparison data are available. The station geometry is varied to include the minimum 1LOC and the maximum 4L4C situations, the 1L1C situation as in Case 2a, and the intermediate 2L1C and 3LOC cases for comparison as indicated by the () symbols in the matrix given in Case 1.

c. The error in altitude for each of the mini-arc epoch points used in Case 3a is calculated by means of a geometric error propagation using range and angle data from ANT. This error propagation assumes a 2 m range measurement uncertainty, a variety of angle measurement uncertainties, and the same survey uncertainties as in Case 3a.

Case 4:

a. A 3-laser, 0-camera (3LOC) situation for a widely spaced laser network having laser stations at Antigua, Key West, and Panama, as was used in Reference 10, is compared with the 3LOC situation in Case 1 having more closely spaced lasers at Antigua, Grand Turk, and Curacao.

b. A 2-laser, 0-camera (2LOC) situation with lasers at Antigua and Trinidad is explored using more optimistic horizontal survey and laser range noise and bias constraints and a higher laser data rate. This is the only case where these survey and laser data constraint parameters are changed.

III. CONSTRAINTS

Realistic station locations and orbital elements are used and the a priori estimates of the uncertainties in the orbit, the survey, the measurements, and the system error model terms, are generally either realistic or conservative. The same values are used for all cases except case 4b. The simulated data are generated at realistic intervals for both the lasers and the cameras. The particulars are as follows:

1. STATIONS

The stations are chosen in the Caribbean Sea area where tracking sites already exist or where they could be easily installed.

	Latitude North	Longitude East	Height (MSL) (Meters)
Antigua	17° 08' 38.5"	298° 12' 25.7"	58
Grand Turk	21° 27' 46.4"	288° 52' 4.4"	28
Trinidad	10° 44' 35.5"	298° 23' 28.9"	792
Curacao	12° 05' 26.2"	291° 07' 43.9"	5

The following two stations are also used in Case 4a:

Key West	24° 0' 0"	278° 0' 0"	0
Panama	9° 0' 0"	281° 0' 0"	0

The stations are ordered for the several cases as follows:

1 Station: Antigua (ANT)

2 Stations: Antigua, Grand Turk (GTK)

3 Stations: Antigua, Grand Turk, Curacao (CUR)

4 Stations: Antigua, Grand Turk, Curacao, Trinidad (TRD)

In the instances where there are both cameras and lasers at the same site, they are assumed collocated at the same position.

2. ORBIT

The orbit assumed is representative of the type of orbit originally considered for the GEOS-C sateilite. However, any trajectory providing a similar tracking geometry will produce similar results.

Osculating elements:

Semi-major axis, a (meters)	= 7817906.7
Eccentricity, e	= 0.025
Orbital plane inclination i, (deg)	= 19.996
Argument of perigee, ω (deg)	= 0.251
R.A. of ascending node, Ω , (deg)	= -0.033
Mean anomaly, M, (deg)	= 53.844

The orbital elements and their a priori constraints in earth-centered, earth-fixed Cartesian coordinates are:

	Elements	Constraints
EPOCH	= 35460 seconds after 0^h GMT	
X(m)	= 3523131.728	1000 meters

	Elements	Constraints
F(m)	= -6489174.888	1000 meters
G(m)	= 2196633.860	1000 meters
$\dot{E}$(m/sec)	= 5643.485	1000 m/sec
$\dot{F}$(m/sec)	= 3361.685	1000 m/sec
$\dot{G}$(m/sec)	= 1410.426	1000 m/sec

At epoch, the satellite topographic coordinates are:

Latitude = 16.673 degrees North

Longitude = 61.501 degrees West

Altitude = 1325537.562 meters

Velocity = 6718.568 m/sec

Velocity azimuth = 77.739 degrees

Flight path angle = 1.291 degrees

The trace of this trajectory over the Caribbean is shown in Figure 1 and the elevation angles vs time for each station are plotted in Figure 2. Note that the pass is almost overhead for Antigua. For this reason, Antigua is always chosen for the one station cases.

3. MEASUREMENTS

Data are simulated for each laser at 40 second intervals and for the altimeter at 50 second intervals for Cases 1, 2, and 4a; at 10 second intervals for the lasers and the altimeter for Case 3; and at 1 second intervals for the lasers for Case 4b. These laser data rates fall between the one per second and one per minute data rates used by the Goddard and SAO lasers respectively. The camera data, right ascension and declination, are generated at 4 second intervals with a total time span of 24 seconds, thus simulating a GEOS 7-flash sequence. The camera data in all cases are equivalent to 1 plate per camera observed near the middle of the laser data span. The altimeter data rates are kept low to minimize the influence of these data on the solution.

Simulated data are generated for the lasers, the cameras, and the altimeter with the following RMS noise values:

Laser range	=	2 meters
Laser angle	=	100 arc seconds
Camera R.A. and Dec.	=	1 arc second
Altimeter	=	10 meters

4. ERROR MODEL

For each station that tracks, a range bias and the station survey are recovered. An altitude bias is recovered for the altimeter. The camera and laser angles are assumed to be free of bias errors, although, for small quantities of data, the biases in these measurements may be as large as the RMS noise values assumed above. The a priori bias uncertainties for the error models are:

Laser range bias		=	2 meters
Altimeter range bias		=	100 meters
Survey:	Longitude, E	=	30 meters
	Latitude, N	=	30 meters
	Height (MSL), V	=	1 meter

IV. RESULTS

All of the computer runs, except for Cases 3c and 4b, were made on the IBM System 360/91 computer using the NAP-II computer program operating in the simulation mode. This mode of operation utilizes the given orbital elements and measurement RMS noise values to generate simulated observations, forms the observation residuals, and outputs the error model recovery statistics for a given tracking situation.

In all of the simulations, recovery is made for the six orbital elements, the survey for each station, a range bias for each laser, and the altimeter bias.

Initially, it was thought it might be necessary to tightly constrain either the orbital elements or the survey for at least one station in order to obtain a convergent solution. This question was investigated for the 4-laser, 0-camera (4LOC) case by obtaining solutions with various orbit and survey constraints (see

Table 1). The first solution used both a more constrained orbit (10 m, 0.5 m/s) and a fixed survey for one of the laser stations (GTK). The second solution held the same orbit constraints (10 m, 0.5 m/s), but allowed for recovery of survey for all 4 stations. This increased the uncertainty in the altimeter bias recovery from 3.13 meters to 3.28 meters. The third solution held the survey for one station fixed and relaxed the orbit constraints (1000 m, 1000 m/s). This further increased the altimeter bias recovery uncertainty to 3.33 meters. Finally, the fourth solution used the relaxed orbit constraints (1000 m, 1000 m/s) and also recovered the survey for all 4 stations. This solution resulted in an altimeter bias uncertainty of 3.42 meters. For these runs, the difference between the most constrained and the least constrained cases was only 0.29 meters in altimeter bias recovery uncertainty. On this basis, it was decided that the a priori orbit and survey constraints could be relaxed with little penalty.

Some additional constrained orbit solutions were run to evaluate the effect of adding cameras and the effect of laser timing uncertainties, (see Table 2). All of the solutions in Table 2 utilized the same orbit constraints (10 m, 0.5 m/s).

The network configuration and constraints for the first two solutions in Table 2 are identical to those for the first two solutions in Table 1, except that now a camera at GTK has been added to the 4 laser network. The first solution used a fixed survey for GTK. Adding a camera at GTK improved the altimeter bias recovery from 3.13 m (Table 1) to 2.68 m (Table 2). For the second solution, allowing for recovery of survey at all 4 sites, adding a camera at GTK improved the altimeter bias recovery from 3.28 m (Table 1) to 3.19 m (Table 2), showing that adding a single camera to the 4 lasers is not as much help when the camera station survey is allowed to adjust.

In solutions 3, 4, and 5 the number of cameras was increased to 2, 3 and 4 respectively, with a corresponding reduction in altimeter bias recovery to 3.04 m, and 2.97 m, and 1.54 m. The addition of CUR camera data in solution 5 was quite helpful, reducing the altimeter bias error to 1.54 m. This was probably because of the earlier acquisition of data by CUR for the chosen trajectory.

In solution 6, the configuration was the same as in solution 5, but now the lasers were allowed to have timing biases with a 1 ms uncertainty. This increased the altimeter bias recovery uncertainty to 2.84 m. For the remaining solutions, timing biases are not allowed, because station clocks can easily be synchronized in the Caribbean to within a few microseconds by a variety of techniques (e.g., Loran-C).

In summary, based on the results with these initial runs, the following assumptions are made in the solutions for the four cases outlined. The orbital elements are essentially unconstrained with an a priori uncertainty of 1000 m in

each position component and 1000 m/s in each velocity component. The station survey is recovered for all stations with a horizontal uncertainty in latitude and longitude of ±30 m for each, and a vertical uncertainty (relative to MSL) of ±1 m.

This assumption for the vertical uncertainty is realistic only near the island tracking site, unless additional data are available. Away from the island, one must know the spatial mean sea level undulations relative to the station. These can be estimated from detailed ocean surface gravity measurements. Also, to some extent, one must know the sea state, the surface barometric pressure, and the surface winds. Many of these data can be made available for the Caribbean. However, the assumption of only a 1-meter error in station height relative to the height of the spatial undulations in mean sea level may be too optimistic. More recent estimates, based on available ocean surface gravity data, quote this error as 2 or 3 meters. On the other hand, the laser range biases are assigned an uncertainty of ±2 m, which is probably too pessimistic, since more recent estimates, based on hardware improvements, quote a value of 0.5 m. Since these two parameters are highly correlated, the a priori estimate of one can be increased by 1.5 m and the other decreased by 1.5 m with probably little effect on the results for the altimeter bias. The altimeter bias is loosely constrained with an uncertainty of ±100 m.

One might anticipate that the altimeter bias recovery from these solutions will be best for the high elevation angle data and will amount to approximately 2.2 m, the root sum square of the 2 m laser range bias uncertainty and the 1 m height uncertainty.

CASE RESULTS

Case 1:

The purpose of this case is to determine how the number of lasers and cameras affects the altimeter bias recovery. Table 3 is a tabulation of the results obtained by varying the number of lasers from a minimum of one to a maximum of four while varying the number of cameras from zero to the number of lasers, as described earlier. From Table 3, the estimated errors in recovery of altimeter bias, orbital elements, and station latitudes and longitudes are plotted in Figures 3, 4, 5, 6, and 7.

From Figure 3 it appears that very little accuracy in altimeter bias recovery is gained beyond the 2 lasers, 2 cameras (2L2C) configuration. This is also evident in the recovery of the orbital elements, shown in Figures 4 and 5 and in the horizontal survey recoveries shown in Figures 6 and 7. Doubling of the tracking equipment from the 2L2C to the 4L4C network gains

only about 0.3 meter accuracy in determination of altimeter bias. In addition, it is highly unlikely that all four stations in the larger network will obtain data on the same pass, due to the weather dependence.

The simplest and cheapest tracking station configuration which meets the 4.1 m requirement, is the 1L1C combination. Next simplest are the 2L1C, 2L2C, and 3LOC configurations.

However, as indicated in Reference 11, the most effective configuration is not necessarily the simplest. Effectiveness involves additional factors such as the probability of obtaining data and the duration of the requisite accuracy in altitude determination.

Estimates of the effect of weather and daylight on the relative probabilities of collecting acceptable altimeter calibration data with the various laser and camera configurations are developed in the Appendix. The results indicate that the 2L2C configuration is the most cost effective configuration having a reasonable probability of obtaining data.

Case 2:

In case 2, it is assumed, for most of the runs, that lasers are available without cameras, and that laser angles provide the only directional information. The laser angle data is assumed to have an uncertainty of 100 arc seconds in azimuth and elevation. Simulations are made for 1, 2, 3, and 4 lasers tracking without cameras, and also for the 4L1C configuration. The results are tabulated in Table 4 and the altimeter bias errors are plotted along with the Case 1 results in Figure 3.

The one station 1LOC case (Antigua) is greatly improved by using the laser angles rather than the laser ranges alone. The altimeter bias uncertainty improves from ±38.7 meters to ±4.7 meters with the addition of the laser angles. The importance of the laser angle data in this case due primarily to the high 87° maximum elevation angle of the pass over Antigua. When the one station situation is repeated using the Grand Turk station with laser range and angles, and a maximum elevation angle for the pass of only 54°, the altimeter bias recovery ±25.5 m. The 2LOC case is improved from 5.1 m to 4.4 m by adding laser angle data.

As can be seen from Figure 3, when more than 2 lasers are tracking, the results are not changed by the addition of laser angle data. For only one or two lasers and no cameras, the laser angles are some help, but with camera angles the improvement in altimeter bias recovery is more pronounced.

Case 3:

a. In Case 3a, recovery of the altimeter bias is simulated using laser and camera data from Antigua at various elevation angles. For each of the 14 one-minute mini-arcs between the minimum elevation of 16° and the maximum elevation of 87° over the Antigua station, the state vector, altimeter bias, laser range bias, and station survey are recovered. The recovery uncertainties are given in Table 5. As anticipated, the uncertainty in the altimeter bias decreases as the elevation angle at the station increases. This is illustrated in Figure 8. The asymmetry between the ascending and descending mini-arc altimeter bias recoveries in Figure 8 is due to plotting the bias recoveries at the elevation angle of the beginning of each mini-arc, rather than at a more representative elevation angle near the middle of each mini-arc. The best mini-arc altimeter bias recovery for the 1L1C case is worse than the 1L1C altimeter bias recovery over the whole arc in Case 1 because there are fewer observations in the mini-arc with which to determine the 11 unknown parameters.

b. In Case 3b, the objective is to determine the dependence of the altimeter bias recovery on elevation for combinations of stations. The computer simulations vary the equipment from the maximum 4L4C case to the minimum 1LOC case with several intermediate cases. An independent altimeter bias is recovered for most of the 14 mini-arcs. The orbit, survey, and bias parameters are recovered over the whole pass. This, in effect, gives the uncertainty of the altimeter bias recovery as a function of the network elevation angle and represents the situation when only short spans of altimeter data are obtained.

The results are given in Table 6 and Figure 9. The five curves in Figure 9 represent the altimeter bias uncertainty as a function of time. The elevation angles at each station as a function of time are given in Figure 2. Indicated on Figure 9 are the times of maximum elevation for the stations. These results show the slight advantage for the 1L1C case of recovering most of the parameters over the whole pass rather than over each mini-arc as in Case 3a. The plots also indicate that the larger the network and the better the tracking geometry the better the altimeter bias recovery at lower elevation angles. In the area of maximum elevation, the 4-station network provides only 0.5 meter better accuracy than the 1-station alone, provided the laser angles at the single station are used. Without the angle data the single station results are much worse, as can be seen in Table 6.

c. In Case 3c, a simpler approach is employed. For the same trajectory points used in Case 3a, the altitude error is determined through a geometric error propagation, assuming a survey uncertainty at ANT of (E, N, V) =

(30, 30, 1) m, a range measurement uncertainty of 2 m, and an angle measurement uncertainty of either 1, 2, 4, 10, or 100 arc-sec. The results are shown in Figure 10. Again, it is evident that the altitude is determined best at the highest elevation angles and at these angles is not very dependent on the angular accuracy. For the lower elevation angles the altitude is better determined with the better angles.

Case 4:

a. In Case 4a, the trajectory is tracked by 3 lasers at Antigua, Key West, and Panama. All recovered parameters and constraints are the same as in Case 1 (Table 3), where the same trajectory is tracked by the 3 more closely spaced lasers at Antigua, Grand Turk, and Curacao.

The results are given in Table 7, along with the earlier results from Table 3 for comparison. The ANT, KWT, PAN network achieves an altimeter bias recovery of 4.13 m compared to 3.80 m with the ANT, GTK, CUR network. Thus, for this set of inputs, the simulations achieve a 0.33 m better altimeter bias recovery with the more closely spaced network.

Both network results are dependent on the inputs and constraints. With a more constrained orbit (10 m, 0.5 m/s), the ANT, KWT, PAN network achieves a 3.33 m altimeter bias recovery. With a more constrained horizontal survey of, say, 5 m rather than 30 m, this network would undoubtedly improve even further, but this run was not attempted.

Both network results are also dependent on the high elevation angle data from Antigua for the chosen trajectory. For example, if TRD replaces ANT in the closely spaced network, the highest elevation angle data now comes from CUR at 74°, and the altimeter bias recovery, even for the constrained orbit case (10 m, 0.5 m/s), deteriorates to 5.6 m.

b. In Case 4b, the ORAN orbital error propagation program is used to identify the critical error sources in the determination of satellite height with simultaneous data from 2 lasers and no cameras (2LOC), and with more optimistic constraints.

The same orbital elements are used, but the epoch is changed to bring the trajectory approximately midway between the 2 lasers at ANT and TRD, providing 18 minutes of simultaneous tracking above 5°. The laser data rate is increased to one per second and the rms noise and bias a priori sigmas are both decreased to 1 m. The TRD survey is held fixed, and the ANT a priori survey error is set at (E, N, V) = (6, 6, 2) m, rather than the previous (30, 30, 1) m. In this case the gravity field errors are also

modelled, using an a priori error estimate of 1 part in 10^6 for GM, and the full difference (except for GM) between the SAO-M1 and the SAO COSPAR coefficients in the spherical harmonics expansion for the gravity potential.

The results near the beginning, middle, and end of the pass are given in Table 8. Again, the satellite altitude determination is best near the middle of the pass, where elevation angles are highest. At this point the error in height is 1.64 m, for the more optimistic constraints employed in this error propagation. With the less optimistic constraints used earlier, this compares with an altitude error of 2.2 m for the 1L1C error propagation in Case 3c. No error propagations were done for the 2LOC configuration using the earlier constraints.

When altimeter bias recovery, rather than error propagation, is attempted with the less optimistic constraints as in Cases 1, 2, and 3a, the 2LOC configuration yields a bias recovery of 5.1 m, 4.4 m, and 6.2 m respectively.

To better evaluate the significance of the improvement in altitude determination indicated in the 2LOC ORAN error propagation, the same more optimistic constraints should be applied consistently to error propagations and bias recoveries for the other laser and camera network configurations.

V. CONCLUSIONS

1. Considering the results of all the cases described, the simplest configuration adequate for the altimeter bias determination appears to be the 1L1C combination. Assuming a 50% chance of clear weather, as needed by both the laser and the camera, and a 50% chance of darkness, as needed by the camera, the chance of obtaining data with this combination on random passes is about 25%. A drawback with this configuration, however, is that it provides sufficiently accurate altimeter calibration data only for high elevation passes above about 60°, and only for short durations, up to about 4 minutes.

2. Adding more lasers and cameras improves the accuracy of the bias determination, extends the accuracy over a longer part of the pass and to lower elevation angles, and increases the chances of obtaining data.

3. The 2LOC configuration, with the superior lasers and accurate relative station surveys indicated in Case 4b, is the next simplest configuration which is adequate. But, for realistic horizontal survey uncertainties, this configuration is probably less accurate than the 1L1C configuration for a high elevation pass. Assuming as before, a 50% chance of clear weather at either station, with no intersite weather correlation, and with no dependence on darkness, the chance

of obtaining data simultaneously from these stations is about 25%, the same as for the 1L1C case.

4. By adding a camera to each of the 2 laser stations, we achieve a 2L2C configuration, which includes the acceptably accurate 2LOC and two 1L1C configurations. With the same 50% assumptions regarding the weather and darkness, the chance of obtaining data from the 2LOC subset is 25% as before, with half of these passes in darkness and suitable for data collection by the more accurate 2L2C network. In addition, there are cases when either one or the other 1L1C station can observe, increasing the overall probability of useful data collection to 50%, as shown in the Appendix. On the basis of the results of this simulation, the 2L2C configuration is probably the most effective combination from the standpoint of cost, accuracy, and probability of useful data acquisition.

VI. RECOMMENDATIONS

1. A network of two stations, each having a laser and a collocated camera (2L2C configuration), and situated for simultaneous observations (about 500 to 1000 kilometers apart) is recommended as a basis for a satellite altimeter calibration such as that anticipated on GEOS-C.

2. Some of these cases should be repeated using more optimistic horizontal survey and other constraints such as were used in Case 4b. This would benefit the multiple station solutions somewhat.

3. The effect of using Doppler data in the short arc solutions should be investigated. Such data will be available on GEOS-C in the Caribbean Sea area.

4. The effect of using data from other ground stations on longer arcs, as described in reference 12, should be further investigated using a more optimistic assumption for the gravity field errors. Also the separately examined range, range rate, and angle data should be tried in various combinations.

5. The effect of using satellite-to-satellite tracking, as described in references 13 and 14, should be further investigated using a realistic assumption for the gravity field errors. This technique seems to be potentially very accurate, provided the orbital arc extends over at least one revolution. This technique, because of its coverage where there are no ground stations, is valuable in conjunction with the altimeter for monitoring the altimeter spacecraft motions and thereby helping to separate variations in the altimeter data due to spacecraft motion from those due to ocean topography. However, since the satellite-to-satellite technique has not yet been evaluated using real data, it would be risky to rely on this technique alone for the GEOS-C satellite altimeter calibration.

REFERENCES

1. Berbert, John H., and Parker, Horace C., "Comparison of C-Band, SECOR, and TRANET with a Collocated Laser on 10 Tracks of GEOS-2," GSFC X-514-68-458, November 1968.

2. Parker, H., Carney, D., and Berbert, J., "Geodetic Systems Intercomparisons Based on 35 GEOS-2 Tasks Taken During the W.I.C.E.," Proceedings of the GEOS-2 Program Review Meeting, June 1970.

3. Stanley, H. R., "Calibration and Evaluation of AN/FPQ-6 Radar Utilizing GEOS-II Satellite, A Status Report," NASA Wallops Station Document X-16-68-1, August 1968.

4. Berbert, J., Hlavin, J., and Reich, R., "Laser/Laser Comparisons from the GORF, ARLACO, and GOLACO Tests," Proceedings of the GEOS-2 Program Review Meeting, June 1970.

5. Pearlman, M., Lehr, G., Mendes, G., and Wolf, M., "A Two-Laser Collocation Experiment," Proceedings of the GEOS-2 Program Review Meeting, June 1970.

6. Hlavin, J., and Berbert, J., "Carnarvon Laser Collocation Experiment (CALACO)," Proceedings of the GEOS-2 Program Review Meeting, June 1970.

7. Rawlinson, F., Harris, D., Oosterhout, J., and Berbeft, J., "The Jupiter Camera Intercomparison Test," Proceedings of the GEOS-2 Program Review Meeting, June 1970.

8. Rados, R., "Project Plan for Geodetic Earth Orbiting Satellite (GEOS-C) (Combined Phase C and D)," February 1971.

9. Berbert, J., and Loveless, F., "Altimeter Bias Recovery from Range and Angle Observations," Proceedings of the GEOS-2 Program Review Meeting, June 22-24, 1970.

10. Vonbun, F. O., Memorandum, "Calibration of the Radar Altimeter for GEOS-C," February 4, 1970.

11. Berbert, J., Memorandum, "GEOS-C Altimeter Calibration and Systems Intercomparison," September 17, 1970.

12. Marsh, J. G., "Tracking Accuracy Studies of GEOS-C Orbits for Altimetry Using Radar and Optical Data," GSFC X-552-70-136, February 1970.

13. Felsentreger, Theodore L., Grenchik, Thomas J., and Schmid, Paul E., "Geodetic Earth Orbiting Satellite (GEOS-C) - Applications Technology Satellite (ATS-F) Tracking Experiment," GSFC X-552-70-96, March 1970.

14. Vonbun, Dr. F., "The ATS-F/Nimbus-E Tracking Experiment," Paper presented at IAU Symposium #48 "Rotation of the Earth," Morioka, Japan, May 9-15, 1971.

15. Harris, D., "GEOS-1 and GEOS-2 MOTS Camera Operations, Data Analysis and Experiments," Proceedings of the GEOS-2 Program Review Meeting, June 22-24, 1970.

APPENDIX

PURPOSE:

To estimate the effect of weather and daylight on the probability of useful data collection by various laser and camera configurations for altimeter calibration purposes.

Assumptions:

1. All configurations more complex than 1LOC can obtain useful data for altimeter calibration purposes (based on Case 1 and 4b results).

2. Satellite passes occur with equal probability over each station. If a pass is above the elevation horizon for one station, it is above this horizon for the others.

3. Daylight (L) or night (N) passes occur with equal probability P(L) = P(N) = 0.5. If a pass is light or night for one station, it is the same for the others.

4. The weather correlation between stations is assumed to be zero. Transparent (T) or Opaque (O) passes occur with equal probability, P(T) = P(O) = 0.5. A second case with probability P(T) = 0.4, P(O) = 0.6, which is more representative of the GEOS-1, 2 results with MOTS cameras in the Caribbean (reference 15) is also examined.

DATA COLLECTION PROBABILITIES

For the equally likely probabilities chosen for transparent or opaque skies, the desired data collection probabilities for the various station configurations can be derived as the outcome of coin tossing experiments, where the coins are labelled transparent (T) or opaque (O), rather than heads or tails. Furthermore, when cameras are involved and darkness is a factor, the equally likely probabilities chosen for darkness or daylight can be represented as another coin in the experiment labelled night (N) or light (L).

One Station

Network A_o = 1LOC (Data not adequate)

This network requires transparent sky passes to acquire data. The equally likely coin toss outcomes are T or O. Thus $P(A_o) = P(T) = 1/2$.

Network A_1 = 1L1C (Simplest case with adequate data)

This network requires both night passes and transparent sky passes in order to acquire data. The equally likely outcomes, when tossing two coins, one labelled N or L, the other T or O are:

N T

N O

L T

L O

The desired result (N, T) has a probability $P(A_1) = P(N, T) = 1/4$

Two Stations

Network B_0 = 2LOC

This network requires transparent sky passes at both laser sites simultaneously, but is independent of whether the passes are day or night. The equally likely outcomes when tossing two coins, both labelled T or O are:

T T

T O

O T

O O

$P(B_0) = P(T, T) = 1/4$

Network B_1 = 2L1C

This network includes both the 2LOC and the 1L1C cases considered above. Considering the night and light passes separately, the possible weather outcomes at the two sites are:

Night (2L1C or 1L1C)	Light (2LOC)
T T	T T
T O	T O
O T	O T
O O	O O

At night, acceptable data can be obtained with the 2L1C systems if it is clear at both sites, or with the 1L1C systems if it is clear at the site with the camera. It is implicitly assumed that at night a possible 2LOC pass is equivalent to a 2L1C pass, since both cases require the same clear skies. $P(B_1/N) = P(T, T) + P(T, O) = 1/4 + 1/4 = 1/2$

In the day passes, acceptable data can be obtained with the 2LOC systems if it is clear at both sites. $P(B_1/L) = P(T, T) = 1/4$

The total probability of obtaining data with this network is:

$$P(B_1) = P(B_1/N)P(N) + P(B_1/L)P(L) = (1/2)\ (1/2) + (1/4)\ (1/2) = 3/8$$

Network B_2 = 2L2C

Since this is still a two station case, the possible weather outcomes given above apply. On the night passes, acceptable data can be obtained with the 2L2C systems if it is clear at both sites, or with either of the 1L1C systems, if it is clear at either site. $P(B_2/N) = P(T, T) + P(T, O) + P(O, T) = 3/4$

$P(B_2/L) = 1/4$ as before

$$P(B_2) = P(B_2/N)P(N) + P(B_2/L)P(L) = 3/4 \cdot 1/2 + 1/4 \cdot 1/2 = 1/2$$

Three Stations

Proceeding as above the day or night possible weather outcomes are:

T TT

T TO

T OT

T OO

O TT

O TO

O OT

O OO

Network C_0 = 3LOC

This requires clear weather at all three sites or at any two (2LOC) sites for adequate data, day or night.

$$P(C_0) = P(T,T,T) + P(T,T,O) + P(T,O,T) + P(O,T,T) = 1/8 + 1/8 + 1/8 + 1/8 = 1/2$$

Network C_1 = 3L1C

The night passes can provide data for the 3L1C, 2L1C, 2LOC, or 1L1C systems and therefore require clear weather at all three sites, or at any pair of sites, or at the camera site alone.

$$P(C_1/N) = P(C_0/N) + P(T,O,O) = 1/2 + 1/8 = 5/8$$

The day passes provide data for the 3LOC or 2LOC systems as above.

$$P(C_1/L) = P(C_0) = 1/2$$

$$P(C_1) = P(C_1/N)P(N) + P(C_1/L)P(L) = 5/8 \cdot 1/2 + 1/2 \cdot 1/2 = 9/16$$

Network C_2 = 3L2C

Proceeding as above

$$P(C_2/N) = P(C_1/N) + P(O,T,O) = 5/8 + 1/8 = 3/4$$

$$P(C_2/L) = 1/2 \text{ again}$$

$$P(C_2) = P(C_2/N)P(N) + P(C_2/L)P(L) = 3/4 \cdot 1/2 + 1/2 \cdot 1/2 = 5/8$$

Network C_3 = 3L3C

$$P(C_3/N) = P(C_2/N) + P(O,O,T) = 3/4 + 1/8 = 7/8$$

$$P(C_3/L) = 1/2$$

$$P(C_3) = P(C_3/N)P(N) + P(C_3/L)P(L) = 7/8 \cdot 1/2 + 1/2 \cdot 1/2 = 11/16$$

Four Stations

Network D_0 = 4LOC

This requires clear weather for any two of the four sites. There are 16 possible weather events, the 8 previously given for 3 stations when the fourth station is clear, and these 8 again when the fourth station is cloudy.

$P(D_0) = 7/16 + 4/16 = 11/16$

Network D_1 = 4L1C

$P(D_1/N) = P(D_0/N) + P(T,O,O,O)$

$= 11/16 + 1/16 = 3/4$

$P(D_1/L) = P(D_0/L) = 11/16$

$P(D_1) = P(D_1/N)\ P(N) + P(D_1/L)P(L) = 3/4 \cdot 1/2 + 11/16 \cdot 1/2 = 23/32 = P(D_0) + 1/32$

Network D_2 = 4L2C

$P(D_2/N) = P(D_1/N) + P(O,T,O,O) = 3/4 + 1/16 = 13/16$

$P(D_2L) = P(D_0/L) = 11/16$

$P(D_2) = 13/16 \cdot 1/2 + 11/16 \cdot 1/2 = 3/4 = P(D_1) + 1/32$

Network D_3 = 4L1C

$P(D_3) = P(D_2) + 1/32 = 25/32$

Network D_4 = 4L4C

$P(D_4) = P(D_3) + 1/32 = 13/16$

The above data probabilities were derived assuming a probability of clear weather P(T) = 50%. By slightly more involved techniques the data probabilities can be derived assuming P(T) = 40%, which is more representative of the probabilities actually experienced with MOTS cameras tracking GEOS-1, 2 from Jamaica and Puerto Rico. The results for both weather probabilities are summarized on the next page.

Note that for P(T) = 50%, the probabilities of obtaining useful data $P(A_1) = P(B_0)$; $P(B_2) = P(C_0)$; $P(C_3) = P(D_0)$. Each time another laser is added to the network, it serves to replace all the cameras in the previous network with respect to data collection capability as defined in this report. Thus, the 25% data

Network		Configuration	Useful Data Probabilities	
			P(T) = 50%	P(T) = 40%
A_1	1 Station	1L1C	1/4 = .250	.200
B_0	2 Stations	2LOC	2/8 = .250	.160
B_1		2L1C	3/8 = .375	.280
B_2		2L2C	4/8 = .500	.400
C_0	3 Stations	3LOC	8/16 = .5000	.352
C_1		3L1C	9/16 = .5625	.424
C_2		3L2C	10/16 = .6250	.496
C_3		3L3C	11/16 = .6875	.568
D_0	4 Stations	4LOC	22/32 = .68750	.5248
D_1		4L1C	23/32 = .71875	.5780
D_2		4L2C	24/32 = .75000	.6312
D_3		4L3C	25/32 = .78125	.6844
D_4		4L4C	26/32 = .81250	.7376

collection probability of a 2LOC configuration can be doubled by adding 2 cameras or 1 laser. Similarly, the 50% probability with a 3LOC configuration can be increased to 68.75% by adding 3 cameras or 1 laser.

For the probabilities with P(T) = 40%, the data collection probabilities are, of course, lower, but the cameras are relatively more effective in improving these probabilities.

Assuming the altimeter satellite carries both laser corner reflectors and optical beacons, the 2L2C configuration is probably the most economical ground station configuration having a reasonably large probability for collection of suitably accurate altimeter calibration data and is therefore recommended as the most effective laser and camera network for this purpose.

Table 1

Exploratory Results with Different Survey and Orbit Constraints

Solution	1	2	3	4
Configuration	4LOC	4LOC	4LOC	4LOC
A priori orbit (m, m/s)	10, 0.5	10, 0.5	1000, 1000	1000, 1000
Survey (Fix, Find)	1, 3	0, 4	1, 3	0, 4
Alt. Bias H(m)	3.13	3.28	3.33	3.42
Orbit (m, m/s)				
E, $\dot{E}$	1.7, .020	4.3, .04	2.1, .04	9.9, .05
F, $\dot{F}$	5.7, .003	8.4, .01	10.7, .006	17.5, .02
G, $\dot{G}$	8.1, .041	9.0, .01	18.4, .08	25.1, .15
Range Bias, B(m) & Vert. Survey V(m)				
ANT (B, V)	1.5, .97	1.6, .98	1.5, .98	1.6, .99
GTK (B, V)	1.8, -	1.9, .99	1.9, -	1.9, .99
CUR (B, V)	1.7, .99	1.7, .99	1.7, .99	1.8, .99
TRD (B, V)	1.8, .99	1.8, .99	1.8, .99	1.8, .99
Horiz. Survey (m)				
ANT (E, N)	7.2, 27.3	9.4, 27.9	11.3, 27.6	16.0, 28.4
GTK (E, N)	- -	12.3, 19.5	- -	22.0, 20.9
CUR (E, N)	8.3, 13.1	11.2, 16.6	14.7, 15.3	16.9, 20.2
TRD (E, N)	8.8, 9.7	13.5, 10.0	17.1, 17.9	19.0, 23.1

A priori parameter uncertainties for all solutions:

Survey: (E, N, V) = $\pm$(30, 30, 1)m
Laser Range Bias: B = $\pm$2m
Altimeter Bias: H = $\pm$100m

Table 2

Exploratory Results with Different Camera Configurations

Solution	1	2	3	4	5	6
Configuration	4L1C	4L1C	4L2C	4L3C	4L4C	4L4C
Camera sites	GTK	GTK	GTK,ANT or TRD	GTK,ANT,TRD		
A priori Orbit (m, m/s)	10, 0.5	10, 0.5	10, 0.5	10, 0.5	10, 0.5	10, 0.5
Survey (Fix, Find)	1,3	0,4	0,4	0,4	0,4	0,4
A priori Laser Time Bias (ms)						1.0
Alt. Bias, H(m)	2.68	3.19	3.04	2.97	1.54	2.84
Orbit (m, m/s)						
E, $\dot{E}$	1.7, .008	3.5, .080	1.8, .006	1.7, .005	0.6, .002	1.9, .004
F, $\dot{F}$	2.2, .003	4.8, .004	2.4, .003	2.0, .003	0.9, .001	2.0, .002
G, $\dot{G}$	5.8, .016	8.8, .027	3.5, .016	2.3, .014	1.1, .003	2.3, .010
Range Bias, B(m), and Vert. Survey, V(m), Time Bias (run 6 only), T(ms)						T(ms)
ANT (B,V)	1.4, .96	1.6, .98	1.5, .97	1.5, .97	1.3, .94	1.5, .96, .98
GTK (B,V)	1.6 –	1.9, .99	1.9, .99	1.9, .99	1.9, .99	1.9, .99, .98
CUR (B,V)	1.7, .99	1.7, .99	1.7, .99	1.7, .99	1.7, .99	1.7, .99, .98
TRD (B,V)	1.8, .99	1.8, .99	1.8, .99	1.8, .99	1.8, .99	1.8, .99, .98
Horiz. Survey (m)						
ANT (E,N)	6.1, 26.2	6.4, 27.7	6.0, 27.0	5.9, 26.9	5.5, 24.8	8.0, 26.5
GTK (E,N)	- -	5.7, 6.8	2.9, 5.3	2.6, 5.3	1.7, 4.0	5.8, 5.0
CUR (E,N)	3.6, 17.0	4.9, 11.8	3.5, 11,0	3.3, 10.6	2.5, 8.5	6.2, 10.4
TRD (E,N)	3.2, 7.8	4.2, 9.6	2.6, 6.8	2.4, 6.2	1.6, 4.8	5.7, 6.1

A priori parameter uncertainties for all solutions:

Survey: (E, N, V) = $\pm$(30, 30, 1)m
Laser Range Bias: B = $\pm$2m
Altimeter Bias: H = $\pm$100m
Time Bias (run 6 only): T = $\pm$1ms

Table 3

Case 1

Lasers	4	4	4	4	4	3	3	3	3	2	2	2	1	1
Cameras	4	3	2	1	0	3	2	1	0	2	1	0	1	0
Alt. Bias (m)	2.87	2.99	3.14	3.36	3.42	3.00	3.16	3.40	3.80	3.20	3.50	5.10	3.60	38.70
Orbit (m, m/s)														
E	1.6	1.9	2.1	2.8	9.9	1.9	2.1	2.9	12.9	2.1	3.4	17.6	4.6	250.
F	2.0	2.6	2.7	2.9	17.5	2.6	2.8	3.0	20.1	2.8	3.0	30.1	3.4	90.4
G	2.3	2.8	2.9	6.7	25.1	2.8	2.9	7.4	42.5	2.9	8.1	76.2	13.7	827.
$\dot{E}$	.004	.005	.006	.044	.054	.005	.006	.049	.085	.006	.055	.144	.097	.752
$\dot{F}$	.003	.003	.003	.013	.017	.003	.003	.014	.022	.003	.016	.028	.028	.216
$\dot{G}$	.010	.011	.015	.124	.149	.011	.015	.138	.220	.015	.157	.334	.276	2.09
Range Bias (m)														
ANT	1.5	1.5	1.5	1.6	1.6	1.5	1.6	1.6	1.6	1.6	1.6	1.7	1.7	1.9
GTK	1.9	1.9	1.9	1.9	1.9	1.9	1.9	1.9	1.9	1.9	1.9	1.9	-	-
CUR	1.7	1.7	1.7	1.7	1.8	1.7	1.7	1.7	1.8	-	-	-	-	-
TRD	1.8	1.8	1.8	1.8	1.8	-	-	-	-	-	-	-	-	-
Survey (m)														
ANT E	5.9	5.9	6.1	6.4	16.0	5.9	6.1	6.4	18.5	6.1	6.6	28.9	6.8	29.9
N	26.6	27.0	27.4	28.1	28.4	27.1	27.5	28.3	28.5	27.8	28.6	28.9	28.9	29.9
V	.97	.97	.98	.99	.99	.97	.98	.99	.99	.98	.99	.99	1.0	1.0
GTK E	2.4	2.7	3.1	11.5	22.0	2.7	3.1	12.7	25.9	3.1	14.4	28.8	-	-
N	4.9	5.2	5.7	16.8	20.9	5.3	5.7	18.5	21.9	5.8	20.2	29.4	-	-
V	.99	.99	.99	.99	.99	.99	.99	.99	.99	.99	.99	.99	-	-
CUR E	3.3	3.7	3.7	8.8	16.9	3.8	3.8	9.7	23.4	-	-	-	-	-
N	10.4	10.5	10.9	13.7	20.2	10.6	10.9	14.3	25.2	-	-	-	-	-
V	.99	.99	.99	.99	.99	.99	.99	.99	.99	-	-	-	-	-
TRD E	2.4	2.8	2.8	11.7	19.0	-	-	-	-	-	-	-	-	-
N	6.0	6.1	6.3	8.8	23.1	-	-	-	-	-	-	-	-	-
V	.99	.99	.99	.99	.99	-	-	-	-	-	-	-	-	-

Table 4

Case 2

Lasers*	4	3	2	1[1]	1[2]	4
Cameras	0	0	0	0	0	1
Alt. Bias (m)	3.40	3.66	4.37	4.70	25.5	3.35
Orbit (m, m/s)						
E	8.7	10.6	12.6	18.7	18.4	2.8
F	15.9	18.3	25.8	28.0	99.7	2.9
G	23.2	36.2	55.3	70.1	211.9	6.5
$\dot{E}$	.052	.077	.114	.21	.43	.043
$\dot{F}$	.015	.019	.022	.05	.06	.013
G	.140	.194	.264	.56	.88	.121
Range Bias (m)						
ANT	1.6	1.6	1.7	1.89	-	1.6
GTK	1.9	1.9	1.9	-	1.99	1.9
CUR	1.8	1.8	-	-	-	1.7
TRD	1.8	-	-	-	-	1.8
Survey (m)						
ANT E	14.9	17.2	24.7	26.7	-	6.4
N	28.4	28.4	28.8	29.7	-	28.1
V	.99	.99	.99	.99	-	.99
GTK E	19.6	21.8	22.7	-	29.8	11.2
N	20.4	21.4	27.4	-	29.7	16.4
V	.99	.99	.99	-	.99	.99
CUR E	16.0	21.8	-	-	-	8.6
N	19.6	23.3	-	-	-	13.6
V	.99	.99	-	-	-	.99
TRD E	18.2	-	-	-	-	11.4
N	21.4	-	-	-	-	8.7
V	.99	-	-	-	-	.99

*Laser Range, Azimuth, and Elevation
[1]Antigua was the single station (best case)
[2]Grand Turk was the single station (worst case)

Table 5

Case 3a

Antigua Laser with Camera

Arc No.	1	2	3	4	5	6	7	8	9	10	11	12	13	14
Start time after 09 hrs (min)	44	45	46	47	48	49	50	51	52	53	54	55	56	57
Elevation Angle at Antigua (deg)	15.6	21.0	27.5	35.5	45.6	58.2	73.5	86.7	71.9	57.5	45.7	36.3	28.8	22.7
Alt. Bias (m)	27.2	18.4	18.5	18.2	16.5	12.2	6.4	6.2	11.6	15.9	18.0	18.7	18.8	20.1
Orbit (m, m/s)														
E	10.9	6.3	7.0	8.6	10.1	9.8	6.7	3.3	8.9	14.9	17.8	18.5	18.0	17.9
F	54.8	27.5	25.9	23.1	18.6	12.1	5.8	4.1	4.1	5.5	9.9	14.4	18.2	21.6
G	13.9	8.8	7.5	6.4	5.6	5.1	4.7	4.4	5.3	7.1	8.7	9.8	10.6	14.4
$\dot{E}$	.71	.33	.31	.29	.26	.21	.17	.16	.15	.16	.19	.23	.27	1.5
$\dot{F}$	.95	.09	.11	.15	.21	.26	.28	.27	.28	.27	.25	.23	.20	.43
$\dot{G}$	.71	.54	.48	.43	.38	.34	.31	.30	.32	.36	.40	.46	.53	4.3
Range Bias (m)	1.99	1.99	1.99	1.99	1.99	1.99	1.99	1.99	1.99	1.99	1.99	1.99	1.99	1.99
Survey (m)														
E	29.59	29.54	29.49	29.40	29.03	27.78	26.03	26.02	27.74	29.0	29.39	29.47	29.50	29.53
N	29.97	29.97	29.97	29.97	29.94	29.91	29.83	29.80	29.87	29.94	29.98	29.98	29.98	29.98
V	1.0	1.0	1.0	1.0	1.0	1.0	1.0	1.0	1.0	1.0	1.0	1.0	1.0	1.0

Table 6

Case 3b

Lasers	4	3	2	1	1*	1
Cameras	4	0	1	1	0	0
Alt. Bias (m)						
Arc 1	5.06	6.83	7.68	8.92	-	-
Arc 2	-	-	-	-	8.18	33.62
Arc 3	4.72	5.97	6.42	7.16	-	-
Arc 4	-	-	-	-	6.54	30.44
Arc 5	4.52	5.33	5.43	5.74	-	-
Arc 6	4.49	5.12	5.09	5.26	5.39	29.67
Arc 7	4.50	4.98	4.87	5.01	-	-
Arc 8	4.55	4.93	4.79	5.03	5.14	29.20
Arc 9	4.65	4.96	4.86	5.29	-	-
Arc 10	4.78	5.07	5.04	5.78	5.89	28.55
Arc 11	-	-	-	-	-	-
Arc 12	5.16	5.49	5.72	7.23	7.34	29.37
Arc 13	-	-	-	-	-	-
Arc 14	5.64	6.10	6.65	9.00	9.11	34.80
Orbit (m, m/s)						
E	1.7	13.6	3.6	5.3	10.6	195.7
F	1.9	20.3	2.8	3.3	20.8	96.3
G	2.3	44.5	8.5	14.6	27.0	65.9
Ė	.007	.09	.06	.11	.13	2.7
Ḟ	.003	.03	.02	.03	.04	0.8
Ġ	.010	.24	.17	.29	.37	7.3
Range Bias (m)						
ANT	1.2	1.5	1.7	1.9	1.9	1.9
GTK	1.4	1.5	1.7	-	-	-
CUR	1.3	1.4	-	-	-	-
TRD	1.4	-	-	-	-	-
Survey (m)						
ANT E	6.4	18.5	6.9	7.8	19.2	29.9
N	27.5	29.0	29.1	29.3	29.5	29.9
V	.97	.99	.99	.99	.99	.99
GTK E	2.2	27.2	14.9	-	-	-
N	4.3	22.2	20.7	-	-	-
V	.99	.99	.99	-	-	-
CUR E	3.4	24.8	-	-	-	-
N	8.5	25.0	-	-	-	-
V	.99	.99	-	-	-	-
TRD E	2.3	-	-	-	-	-
N	4.9	-	-	-	-	-
V	.99	-	-	-	-	-

*Laser range, azimuth, elevation

Table 7

Case 4a

Configuration		3LOC		3LOC
Laser Sites		ANT, KWT, PAN		ANT, GTK, CUR
A priori orbit (m, m/s)		1000m, 1000m/s		1000m, 1000m/s
Alt. Bias (m)		4.13		3.80
Orbit (m, m/s)				
E, $\dot{E}$		16.2, .062		12.9, .085
F, $\dot{f}$		20.4, .014		20.1, .022
G, $\dot{G}$		57.4, .143		42.5, .220
Range Bias, B(m) & Vert. Survey V(m)				
(B, V)	ANT	1.6, 0.99	ANT	1.6, .99
	KWT	2.0, 1.00	GTK	1.9, .99
	PAN	1.8, 1.00	CUR	1.8, .99
(E, N)	ANT	28.7, 19.4	ANT	28.5, 18.5
	KWT	22.1, 27.9	GTK	21.9, 25.9
	PAN	24.3, 23.3	CUR	25.2, 23.4

Table 8

Error Contributions Near Beginning, Middle, and End of Pass Case 4b

Error Source	Position Radial (ΔH) (m)	Position Cross (m)	Position Along (m)	Velocity Radial (m/s)	Velocity Cross (m/s)	Velocity Along (m/s)
y/m/d h/m/s						
Time A: 690820-085100.						
GRAVITY	3.31	0.68	2.12	-0.76	-0.23	0.15
GM	-0.79	-0.02	-0.55	0.35	0.00	0.13
ANT RNG BS	-1.17	-2.25	-0.25	0.18	-0.15	-0.02
ANT E	0.31	-28.10	3.08	-0.39	4.84	0.08
ANT N	1.17	11.20	0.38	0.02	1.19	0.01
ANT V	0.82	2.63	0.45	-0.03	0.19	0.01
PSP RNG BS	0.83	2.13	0.54	-0.03	0.17	-0.10
RSS	3.97					
Time B: 690820-090200.						
GRAVITY	-0.14	0.10	0.73	-0.39	0.04	-0.13
GM	-0.00	0.01	0.05	-0.04	0.01	0.06
ANT RNG BS	-0.53	-2.75	-0.15	0.06	-0.01	-0.08
ANT E	0.08	3.84	3.57	-0.32	5.51	0.10
ANT N	-1.00	-2.70	0.99	-0.09	1.57	-0.00
ANT V	1.02	3.27	-0.07	0.06	0.02	-0.01
PSP RNG BS	-0.59	2.78	0.21	-0.12	0.04	-0.07
RSS	1.64					
Time C: 690820-090900.						
GRAVITY	-1.31	0.13	0.97	-0.34	-0.01	0.02
GM	-0.82	0.03	0.60	-0.35	0.00	0.13
ANT RNG BS	-0.53	-2.53	-0.36	-0.02	0.10	-0.08
ANT E	0.38	29.05	3.94	-0.26	4.82	0.08
ANT N	1.10	4.85	1.46	-0.18	1.52	0.01
ANT V	1.35	3.06	-0.74	0.15	-0.11	-0.04
PSP RNG BS	-1.29	2.68	0.40	-0.22	-0.08	-0.01
RSS	2.74					

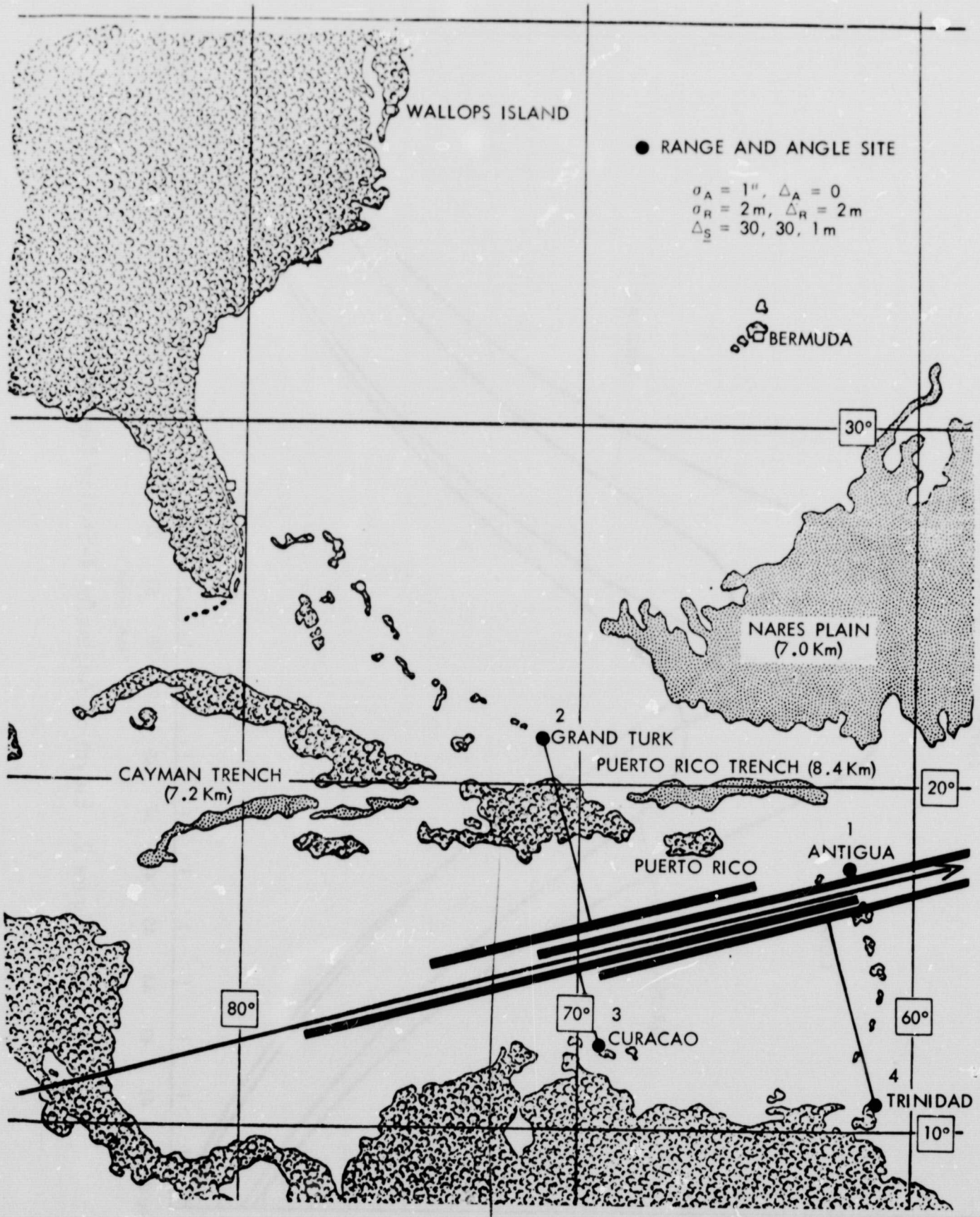

Figure 1. Satellite Ground Trace for a 20° Inclination Orbit

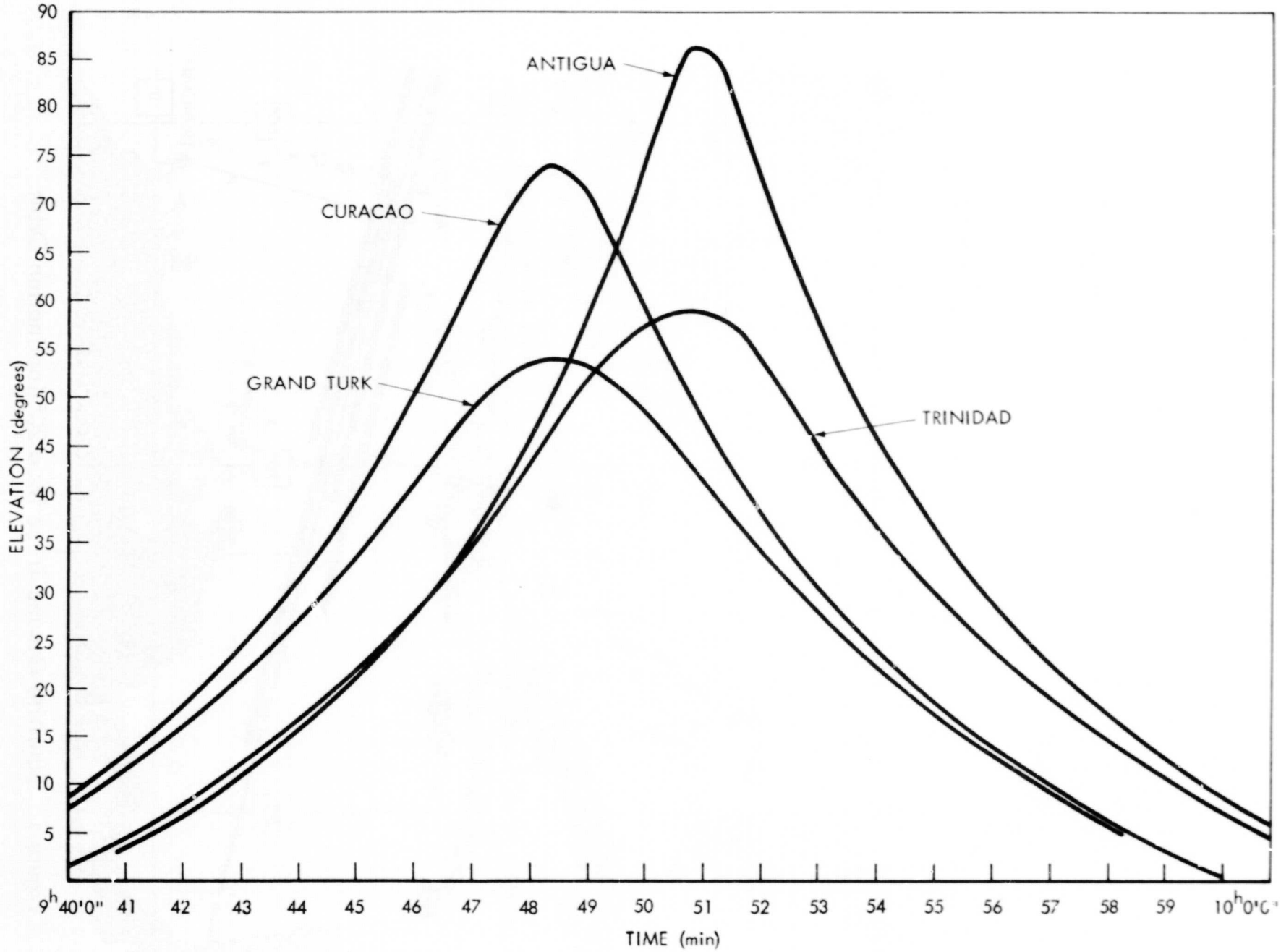

Figure 2. Elevation Angles for 4-Station Network

NOTE: DATA SIMULATED FOR LASERS AND CAMERAS WAS ORDERED BY STATION.

NO. OF LASERS OR CAMERAS	STATION ORDER
1	ANT
2	ANT, GTK
3	ANT, GTK, CUR
4	ANT, GTK, CUR, TRD

⊙ LASER RANGE, AZIMUTH & ELEVATION ANGLE DATA USED

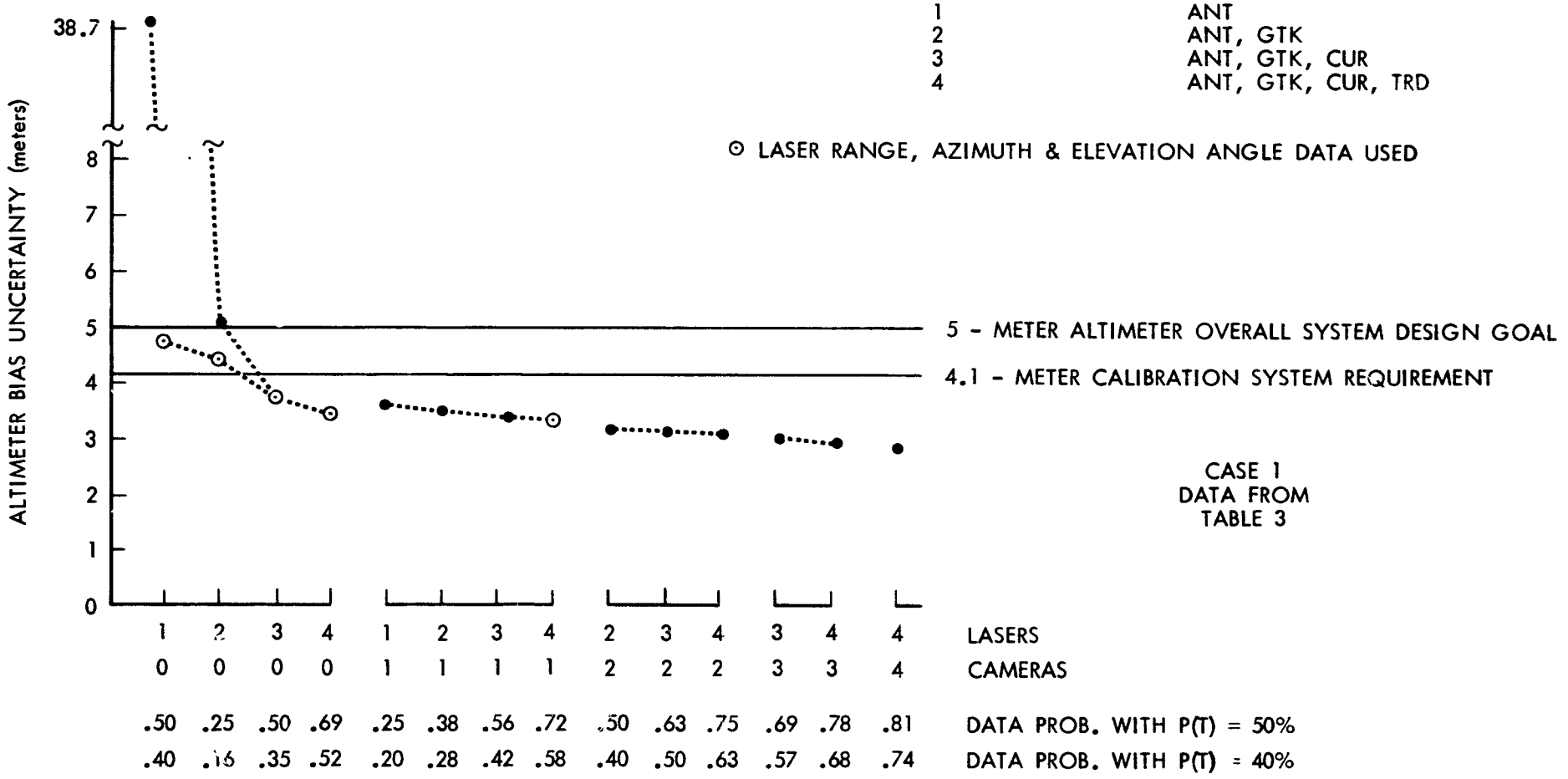

Figure 3. Case 1, and 2, Altimeter Bias Recovery vs Equipment Tracking

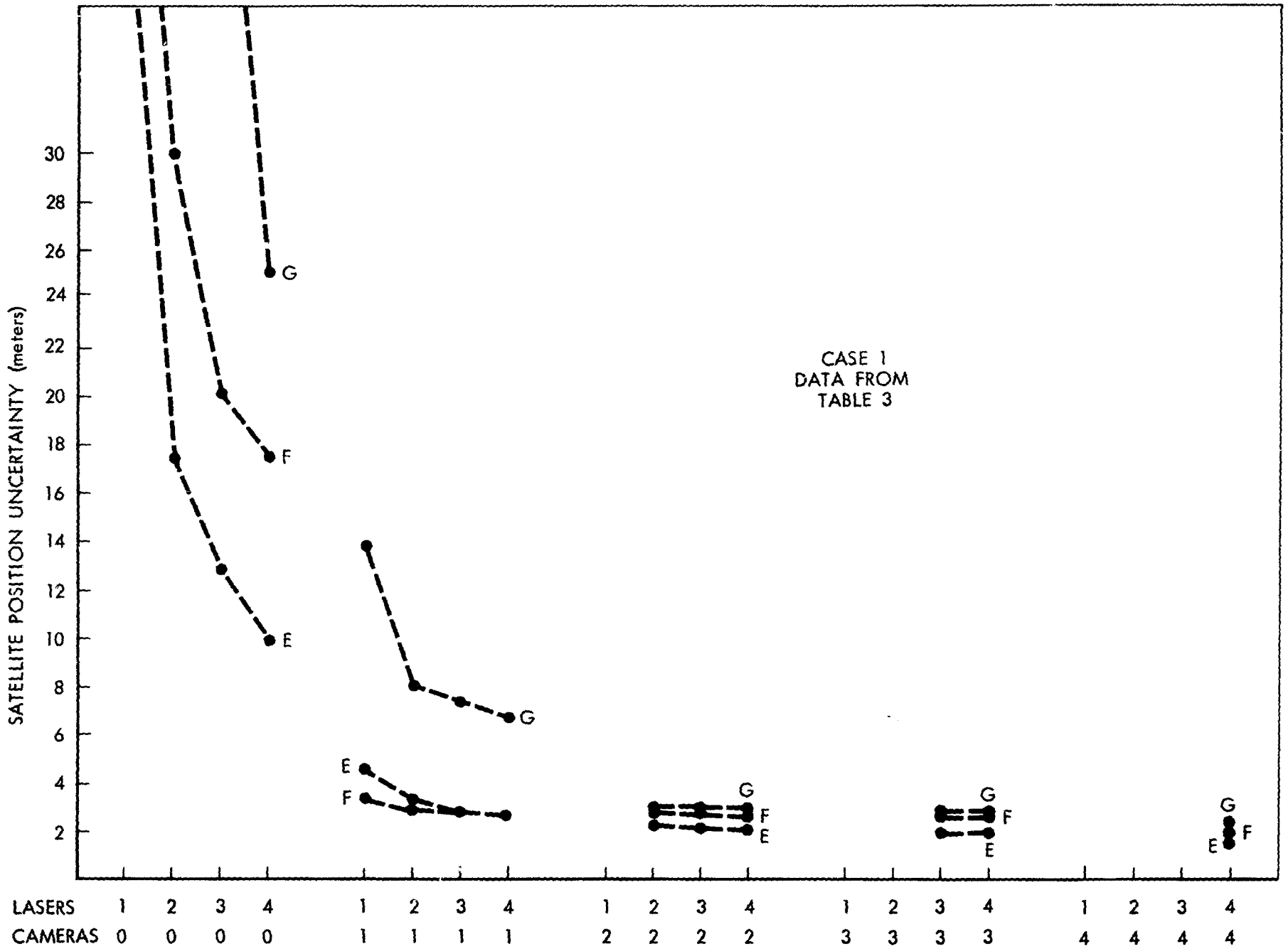

Figure 4. Case 1, Satellite Position Recovery vs Equipment Tracking

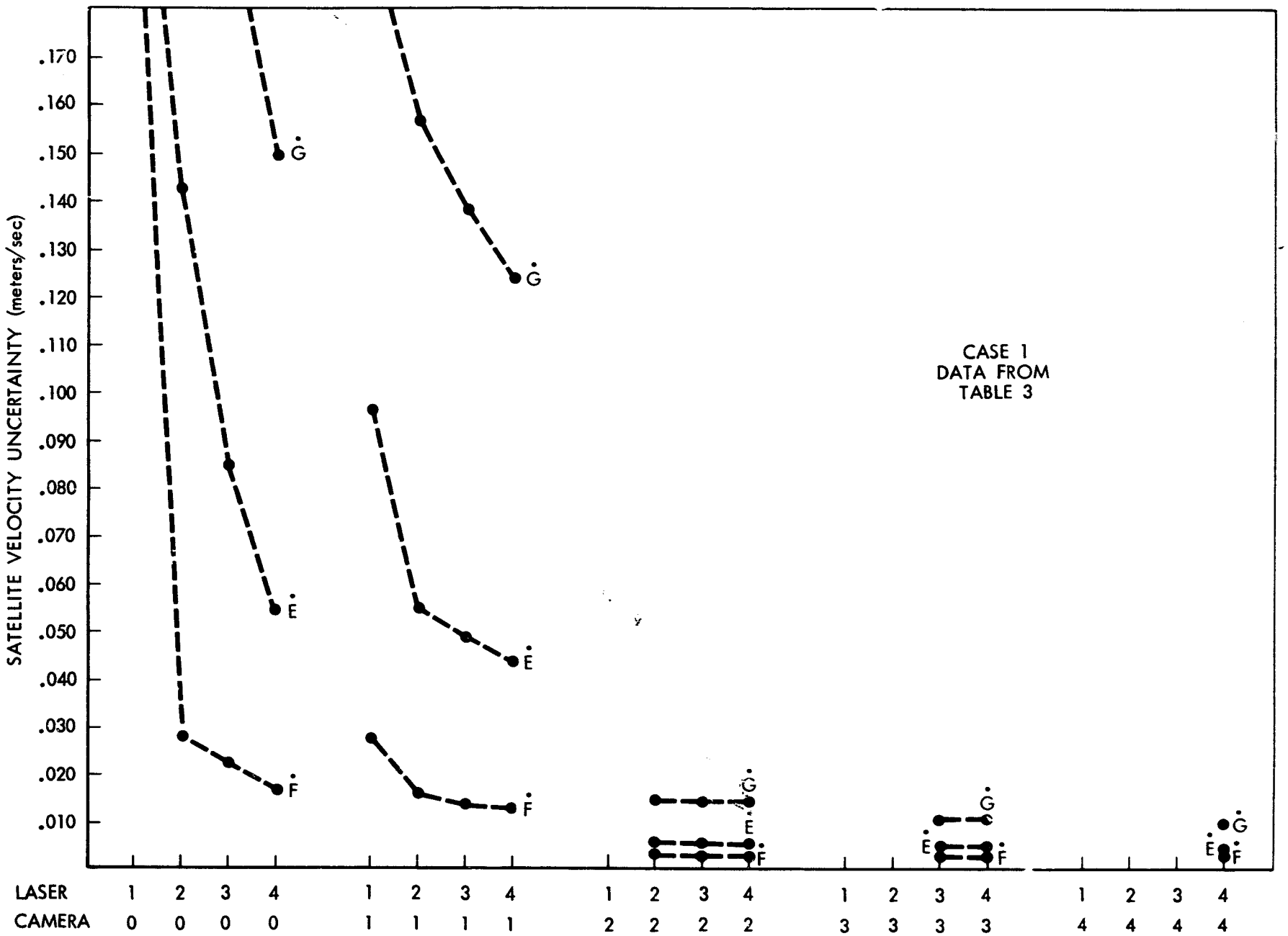

Figure 5. Case 1, Satellite Velocity Recovery vs Equipment Tracking

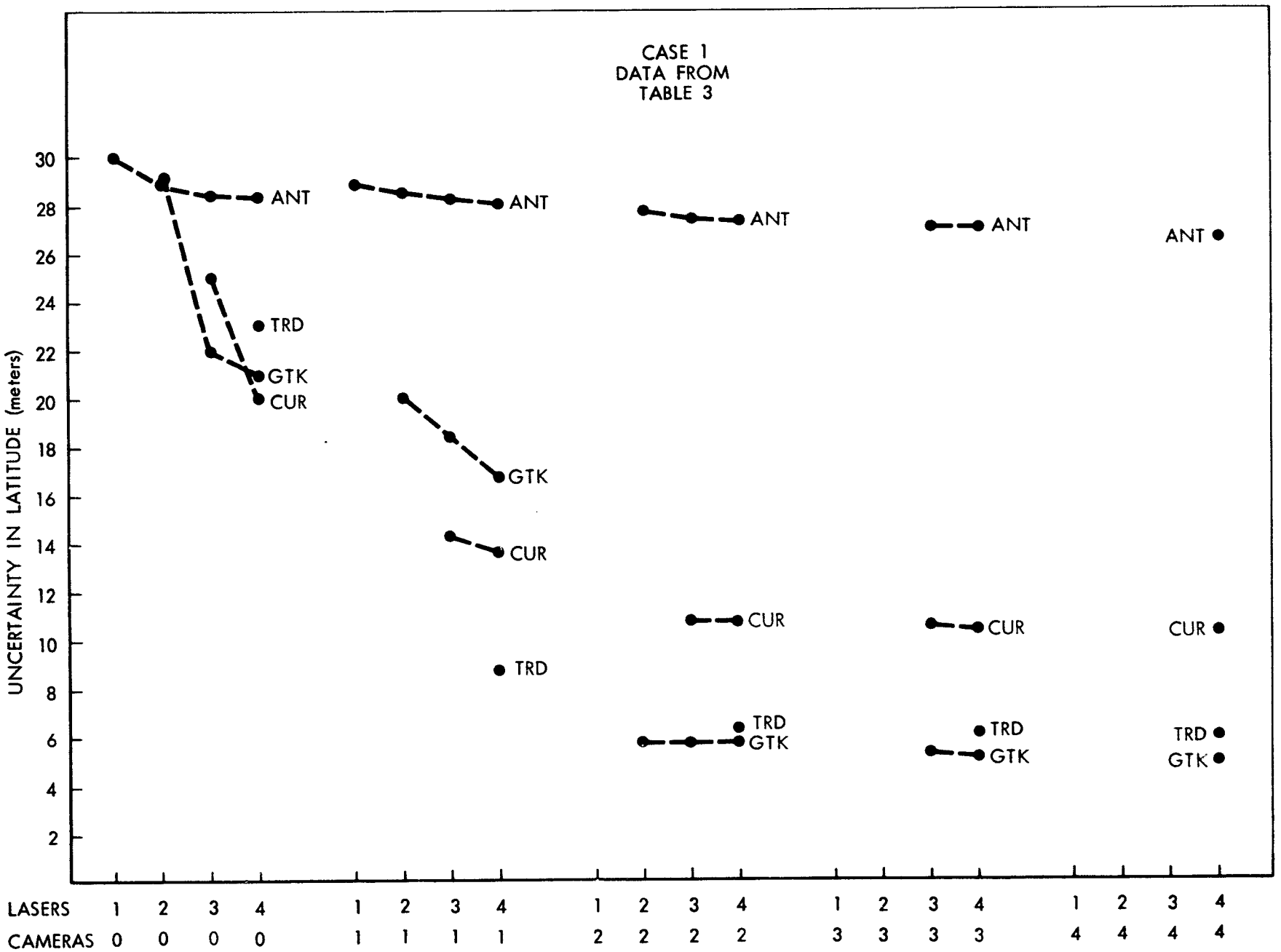

Figure 6. Case 1, Satellite Latitude Recovery vs Equipment Tracking

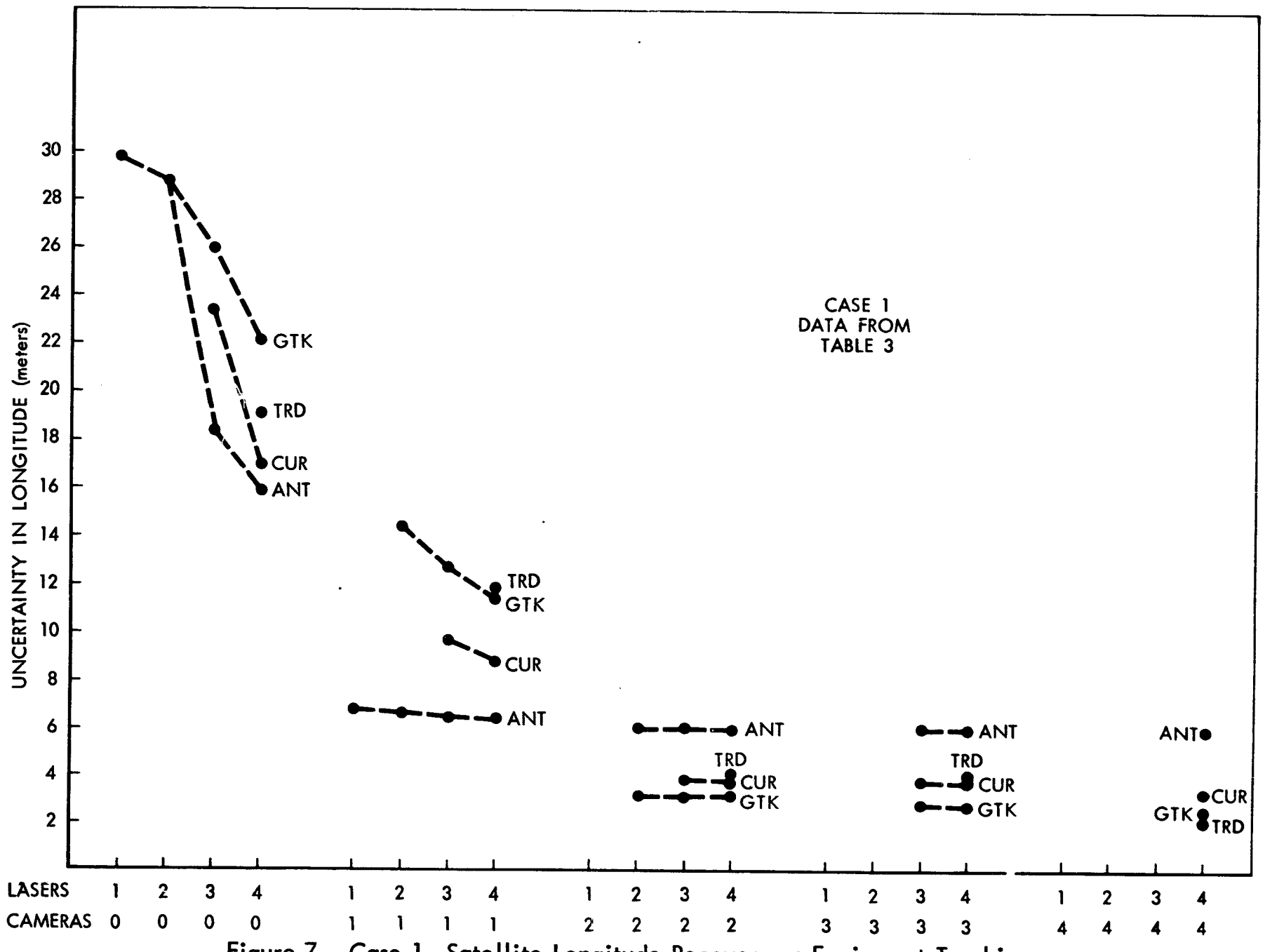

Figure 7. Case 1, Satellite Longitude Recovery vs Equipment Tracking

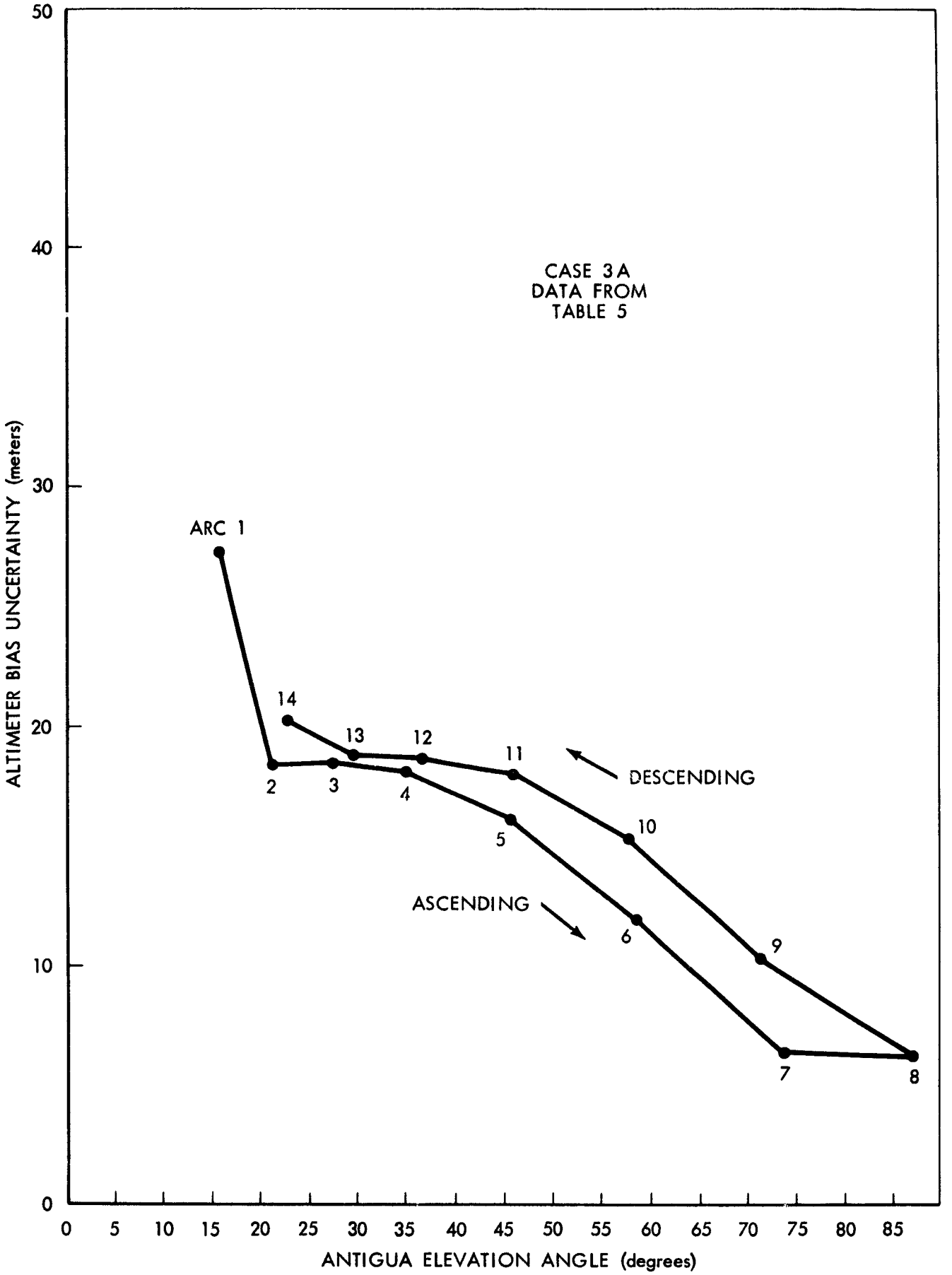

Figure 8. Case 3a, Altimeter Bias Uncertainty vs Elevation Angle

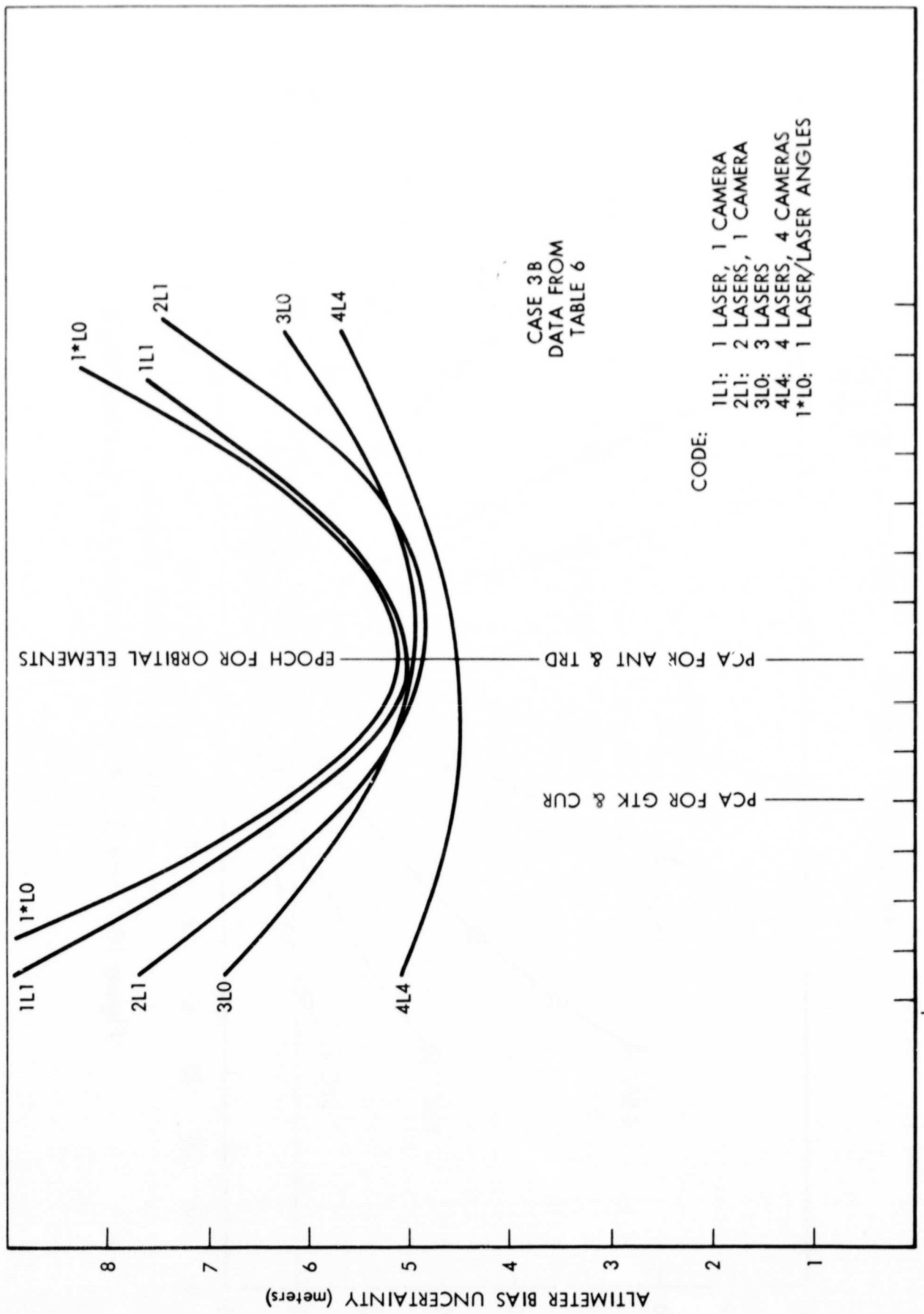

Figure 9. Case 3b, Altimeter Bias Recovery vs Time of Pass

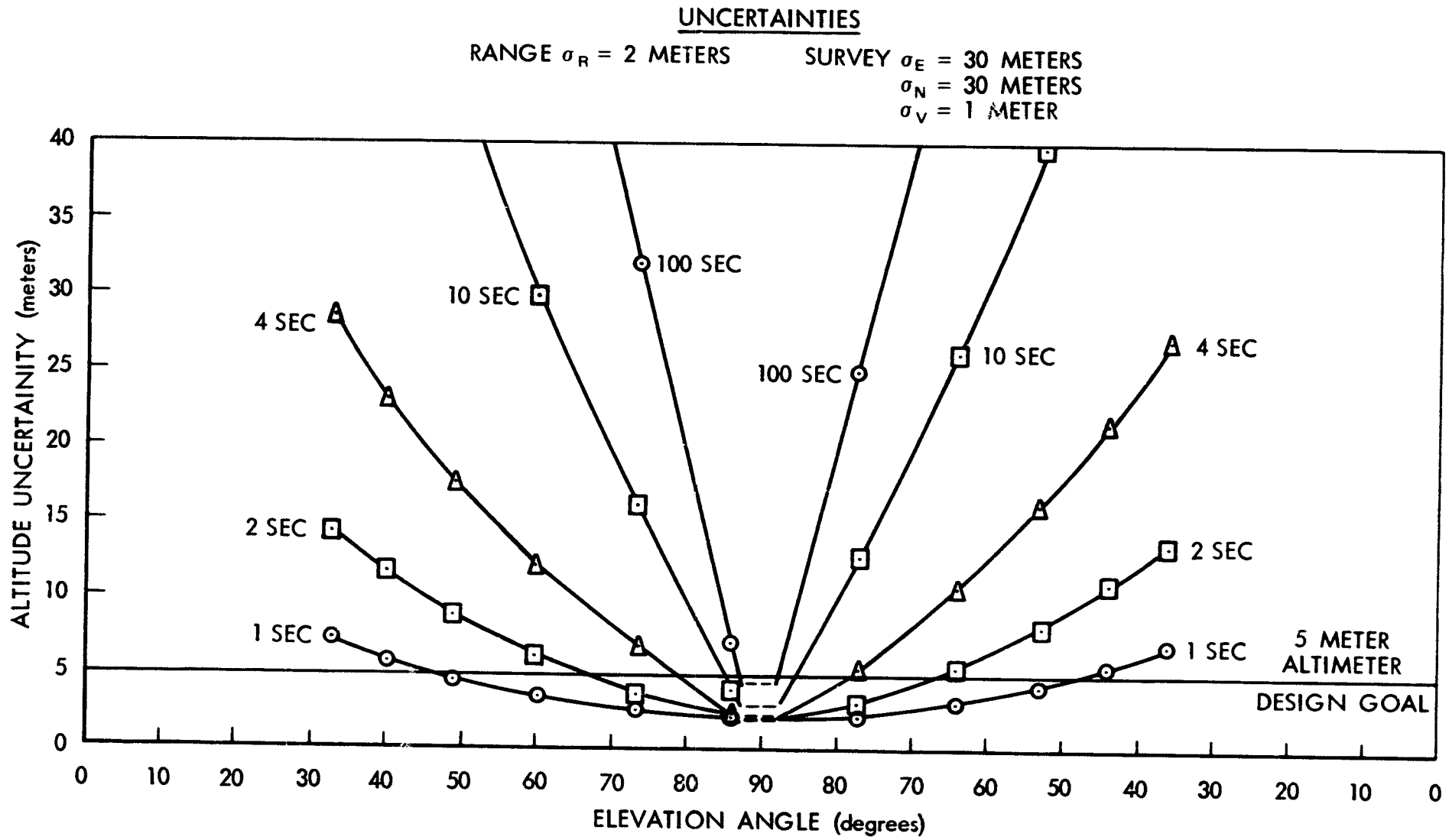

Figure 10. Case 3c, Altitude Uncertainty vs Elevation Angle